METEOROLOGICAL APPLICATIONS
Meteorol. Appl. **18**: 137–154 (2011)
Published online 24 March 2010 in Wiley Online Library
(wileyonlinelibrary.com) DOI: 10.1002/met.187

RMetS
Royal Meteorological Society

An observational study of the exceptional 'Ottery St Mary' thunderstorm of 30 October 2008

M. R. Clark*
Met Office, FitzRoy Road, Exeter, EX1 3PB, UK

ABSTRACT: A small but intense convective system affected parts of east Devon during the early hours of 30 October 2008, producing an estimated 200 mm of precipitation, including locally over 20 cm of hail, within a 3 h period. This exceptional storm and its environment are studied here from an observational perspective. Upper air and satellite observations show that the storm developed within an environment characterized by a trend for increasing instability and dynamic forcing for ascent, associated with an approaching upper level cold pool and small positive potential vorticity anomaly. Analysis of surface observations reveals that convective development was strongly focussed by localized, persistent low-level convergence and moisture convergence in the vicinity of a mesoscale surface low pressure area, which rapidly deepened before becoming slow moving over east Devon. Radar, wind profiler and other available observations are used to describe the development and evolution of the convective system, and to identify some additional factors contributing to the exceptional rain- and hail-fall totals. Finally, the role that real-time, simultaneous analysis of these various observation types could play in nowcasting of localized, extreme rainfall events is discussed.

KEY WORDS devon; flash flood; hail; extreme rainfall; convection; observations

Received 10 November 2009; Revised 30 December 2009; Accepted 15 January 2010

1. Introduction

Between 0000 and 0300 UTC on 30 October 2008 a small, intense area of thunderstorms affected parts of east Devon. Worst affected was the small town of Ottery St Mary, located approximately 15 km east of Exeter (Figure 1). Flash flooding caused significant damage to property, highways and farmland within a highly localized area. A number of people had to be airlifted to safety from their homes or vehicles. In addition to intense rainfall, copious quantities of small hail fell. Deep deposits of hail built up in places, which appeared to augment flooding by obstructing free drainage of water. These waterborne hail deposits accumulated to a depth of over 1 m in a few places, though eyewitness reports suggested that the maximum level depth of lying hail over open, unflooded ground was typically on the order of 10–20 cm in the worst affected areas. There was at least one report of damage to property owing to the weight of accumulated hail. Although river flooding was severe and extensive along the River Otter, much of the damage in the area immediately affected by the thunderstorms appears to have been caused by surface run off and flooding from small watercourses, together with landslips and accumulation of debris. The event appears all the more unusual when it is considered that it occurred within a relatively dry environment, exhibiting much lower values of precipitable water and surface dew point temperatures than have been observed for other documented flash flood events of a similar magnitude in the United Kingdom.

From an observations standpoint, the location of the storm was somewhat fortuitous, since the area affected lies within range of Doppler radar and only 15 km from a wind profiler station. These and other available observations are used to explore the primary factors leading to this exceptional event, to explain why it occurred where it did, and to explain how such a storm was able to occur within a relatively dry environment. This post-event analysis also provides some insight into the role that a multifaceted, high resolution observations network might play in short term (0–6 h) forecasting of small scale, convective events, potentially adding significant value to the output of high-resolution numerical models. This aspect is explored further in Sections 5 and 9. An overview of the areal extent of the exceptional rain- and hail-fall is presented in Section 2. A brief description of the available observations is provided in Section 3. The synoptic and mesoscale situation in which the storm developed is investigated in Sections 4 and 5. Radar and wind profiler data are analysed in Sections 6 and 7. Discussion and Conclusions are given in Sections 8 and 9, respectively.

2. Location and extent of exceptional rain- and hail-fall

A number of damage surveys were undertaken in the area around Ottery St Mary in the days following the storm.

* Correspondence to: M. R. Clark, Met Office, FitzRoy Road, Exeter, EX1 3PB, UK. E-mail: matthew.clark@metoffice.gov.uk

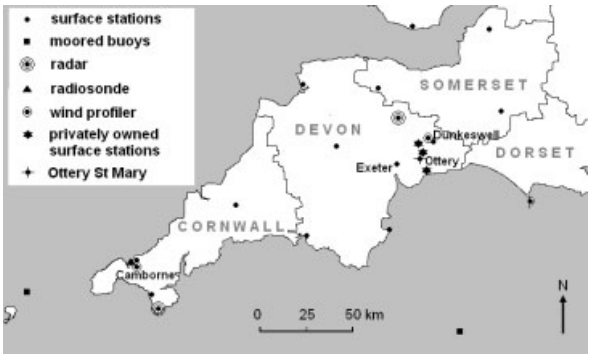

Figure 1. Location of meteorological sensors and observing stations of various types over southwest England, as of October 2008. Locations of other principal places of interest mentioned in the main text are also shown.

The surveys revealed that the worst damage was limited to a very narrow swathe, running from southwest to northeast, and centred on the lower slopes of the west side of the Otter River valley. The most extensive damage (excluding that resulting from the widespread river flooding along the River Otter at locations downstream from Ottery St Mary) occurred within the area bounded by Feniton to the north, Ottery St Mary to the east, Tipton St John to the south and West Hill to the west. Figure 2 shows estimated level hail depths and radar derived rainfall totals, for the 4 h ending 0300 UTC, over this area. The distribution of maximum level hail depths has been estimated from a combination of survey data, eyewitness accounts and information provided by photographs published by the media. Maximum level hail depths exceeded 20 cm, and possibly approached 30 cm. Figure 2 shows that accumulations of 10 ± 3 cm or more appear to have occurred over an area approximately 3 km^2 in size. Accumulations of 5 ± 2 cm appear to have occurred over an area approximately 12 km^2 in size. This area forms an elongated oval with its long axis orientated roughly southwest to northeast, of length approximately 6 km and width just under 3 km at its widest point. Lesser accumulations (i.e. 2 ± 1 cm or more) occurred over a considerably larger, though still localized swathe, which was no more than 5 km wide at its widest point.

The rainfall totals shown in Figure 2 have been obtained from the Met Office Cobbacombe Cross radar, which is located approximately 30 km northwest of Ottery St Mary. It should be noted that the rainfall values shown over much of the area will almost certainly be larger than the true totals. This is because the presence of hail in the radar beam results in very large reflectivity values, leading to potentially large errors in rainfall totals when the standard Z-R (radar reflectivity to rainfall rate) equation is applied (e.g. Austin, 1987; Fulton *et al*., 1998). Nevertheless, the distribution of totals does give a good indication of the location and spatial extent of the extreme rain- and hail-fall event. The swathe of highest totals (>150 mm), in the area between West Hill and Ottery St Mary, agrees very well with the swathe of deepest hail as determined from the damage surveys and eyewitness accounts. Some measure of the overestimation of the radar derived totals can be obtained from comparison of available gauge data with the radar-derived totals. An estimated 3 h rainfall total of 160 mm, for the period ending 0300 UTC, was derived from a 27 h total of 187 mm obtained from a storage gauge located at Kings School, on western edge of Ottery St Mary. This value has a return period of well over 200 years (Met Office, 2008). The location of this gauge is shown

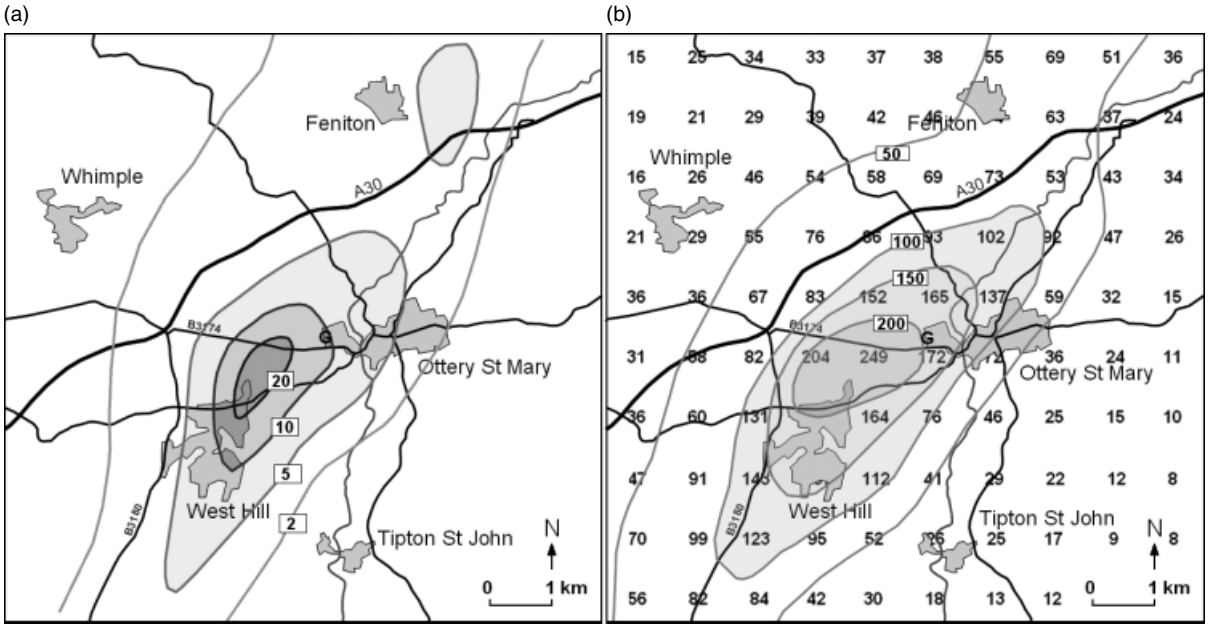

Figure 2. Estimated distribution of maximum level hail depths in centimetres (a) and 1 km^2 resolution radar derived rainfall totals, in mm, for the 4 h period ending 0300 UTC 30 October 2008 (b) over Ottery St Mary and the surrounding area. 'G' denotes location of the King's School rain gauge.

in Figure 2. It can be seen that the gauge lies on the eastern edge of the area with deepest hail fall, where 4 h radar derived totals were close to 200 mm. A check of the 3 h (ending 0300 UTC) radar derived total at this location showed a very similar value, which permits a valid comparison with the estimated 3 h gauge total; 4 h totals were chosen for Figure 2 however, since it was felt that this gave a better representation of the 'storm total' over other parts of the area shown. This gives a gauge-to-radar totals ratio of approximately 4 : 5 at the location of the gauge. A similar ratio applied to the peak radar derived total of 250 mm, located approximately 1 km to the west, would suggest that the highest storm totals were around 200 mm. However, it must be emphasized that a large uncertainty surrounds this value, owing to factors such as gauge measurement error (associated, e.g. with bounce-out of hail from the gauge and possible blocking) and assumptions associated with the interpolation between radar derived rainfall values obtained for adjacent 1×1 km^2.

3. Observations network

Figure 1 shows the measurement locations of the various observation types available for analysis. A number of Met Office surface stations ('synoptic' stations) are spread over the region, from which archived hourly temperature, dew point temperature, wind speed, wind direction and pressure measurements have been analysed. Supplementing the land-based network of surface stations, a smaller number of fixed buoys are located in the English Channel and southwest approaches, from which hourly surface dew point temperature, pressure, wind speed and wind direction data have been analysed. A Met Office Doppler radar is located approximately 30 km northwest of Ottery St Mary, at Cobbacombe Cross, near Tiverton, providing high resolution radar reflectivity and radial velocity data at 5 min intervals. In addition to this, a wind profiler is located at Dunkeswell Aerodrome, just 15 km north-northeast of Ottery St Mary. The close proximity of the wind profiler station to the storm has in this case allowed detailed analysis of a representative environmental vertical wind profile and its variation through the duration of the event. Data are available at a vertical resolution of 200 m and a temporal resolution of 5 min. Radiosonde data are available for 0000 UTC 30 October 2008 from Camborne, west Cornwall. Camborne is located approximately 160 km west-southwest of Ottery St Mary. In this case, data from a number of privately owned surface stations located in the immediate vicinity of Ottery St Mary were also analysed. These data have provided significant added value, increasing the ability of surface analyses to resolve small scale (i.e. approaching storm-scale) variations in surface parameters. Data from three privately owned stations in east Devon have been used; Kerswell, Feniton and Sidmouth (the northern, middle and southern stations, respectively, as shown in Figure 1). It can be seen that, when used together, these various observations comprise a reasonably high resolution and diverse observations network. It will be shown subsequently that, in addition to providing insight into factors leading to this exceptional storm, the data produced by this network might also have contributed to more successful short-term forecasting and warning of this event.

4. Synoptic analysis

Figure 3 shows surface analyses charts for 0000 and 0600 UTC 30 October 2008. At 0000 UTC a broad region of relatively low mean sea level pressure was present over much of western and northern Europe. Within this area, three individual depression centres are shown by the analysis: of most significance to this event was the depression centred close to Pembrokeshire in South Wales. This depression had moved steadily south-southeast through the preceding 24 h. Cyclonic flow in the vicinity of the depression affected almost the whole United Kingdom. Pressure gradients over much of the United Kingdom were weak, however, with south to southeasterly flow present over much of England and Wales to the east of the depression centre. Stronger pressure gradients existed to the west of the depression, along the flank of a large, meridionally elongated anticyclone over the mid-Atlantic. An occluding frontal system, associated with the depression near the United Kingdom, was located over the Bay of Biscay at 0000 UTC, with the triple point located close to the Brest Peninsula of northwest France. The occlusion extended to the north, lying across Devon, Somerset and the southwest of Wales. A band of persistent rain associated with this occlusion had spread slowly eastwards over the southwest of the United Kingdom through the evening of the 29 October. Rainfall rates within the occlusion rain band had been moderate to heavy during the evening (typical rates in the range 2–6 mm h^{-1}) though some weakening and fragmenting of the rain band had occurred by 0000 UTC. The occlusion pivoted cyclonically around the southward moving depression during the period, with the pivot point located close to or over southwest England. As a result, the occlusion became stationary over Devon for a period of several hours, as can also be inferred from radar rainfall imagery.

Figure 4 shows 500 hPa geopotential height and temperature fields for 0000 and 1200 UTC 30 October 2008. At 0000 UTC, a 500 hPa geopotential height minimum was centred over the Irish Sea, approximately 100 km north of the location of the surface depression at the same time (compare with Figure 3). The height minimum lay close to the base of a much larger trough in the 500 hPa height field, which at the analysis time extended northeast from the United Kingdom and northern France towards Scandinavia and beyond. A northerly jet was present to the west of the trough, though flow over much of the United Kingdom, located within the broad trough, was relatively weak. Divergence in the 500 hPa flow was present over extreme south-western United Kingdom, north-western France, and more particularly the Bay of Biscay, under the exit region of the jet.

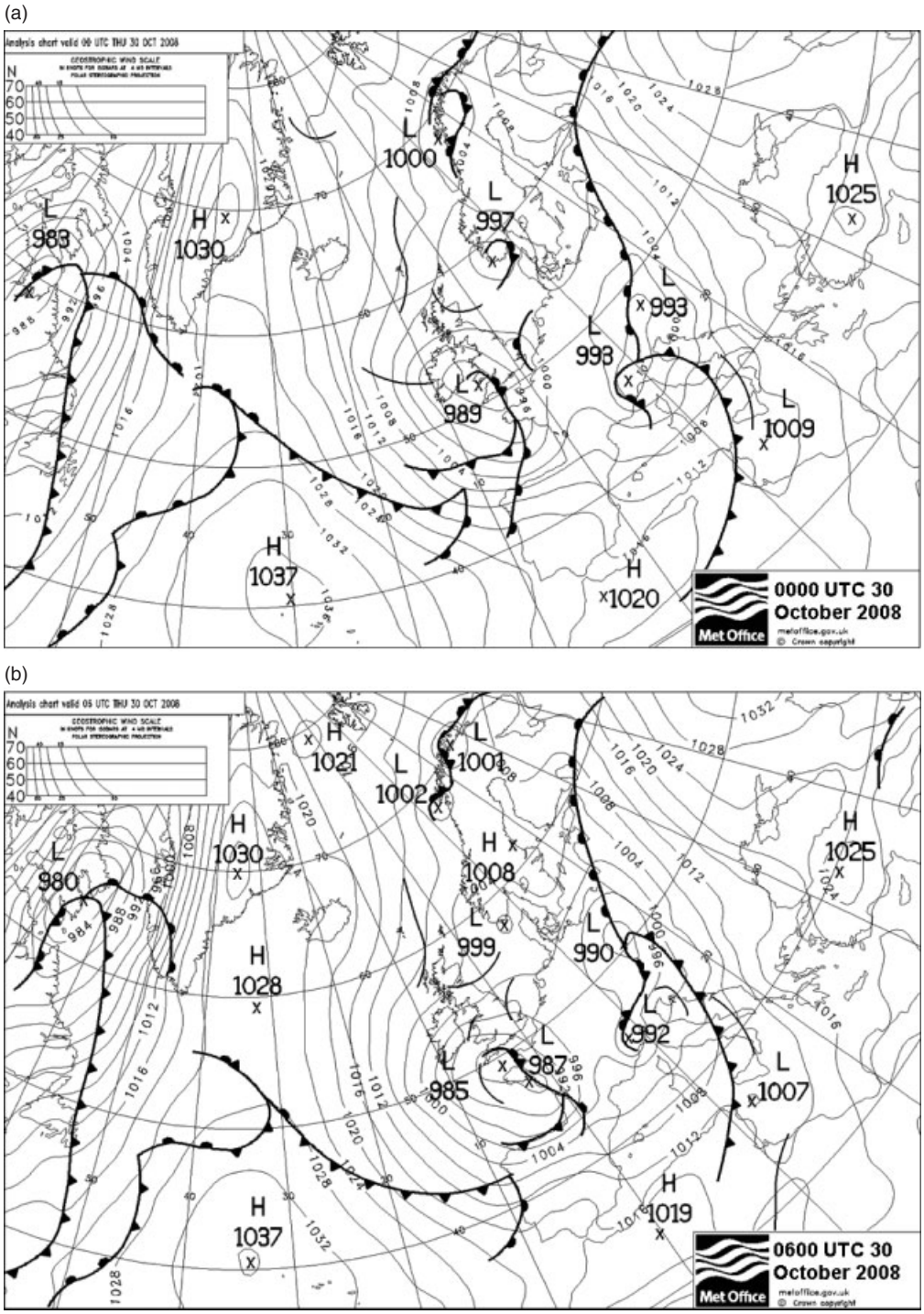

Figure 3. Europe and North Atlantic surface analysis charts for 0000 UTC (a) and 0600 UTC (b). Isobars are drawn at 4 hPa intervals. Surface fronts and troughs are shown by conventional symbols. (Crown Copyright Met Office (2008)).

Analysis charts for earlier times (not shown) reveal that the left exit region of the jet moved south from Ireland in the preceding 12 h as the jet extended south, passing close to west Cornwall around 1800 UTC. The 0000 UTC chart also reveals a small cold pool which was more or less collocated with the 500 hPa height minimum at 0000 UTC, characterized by temperatures of $-30\,^{\circ}\mathrm{C}$ and less. The 500 hPa low and associated cold pool moved slowly south over southwest England, and was centred in the vicinity of the Brest Peninsula of northwest France by 1200 UTC 30 October. Easterly 500 hPa flow is indicated to the north of the feature over the southern United Kingdom by this time.

Figure 5 shows a sequence of Meteosat Second Generation (MSG) 6.2 μm water vapour images. The images can be used to identify moist and dry regions in the middle to upper troposphere, with darker regions indicative of lower humidity at these levels. The dark regions also indicate positive potential vorticity anomalies in the upper troposphere (see, e.g. Georgiev, 1999). At 2200

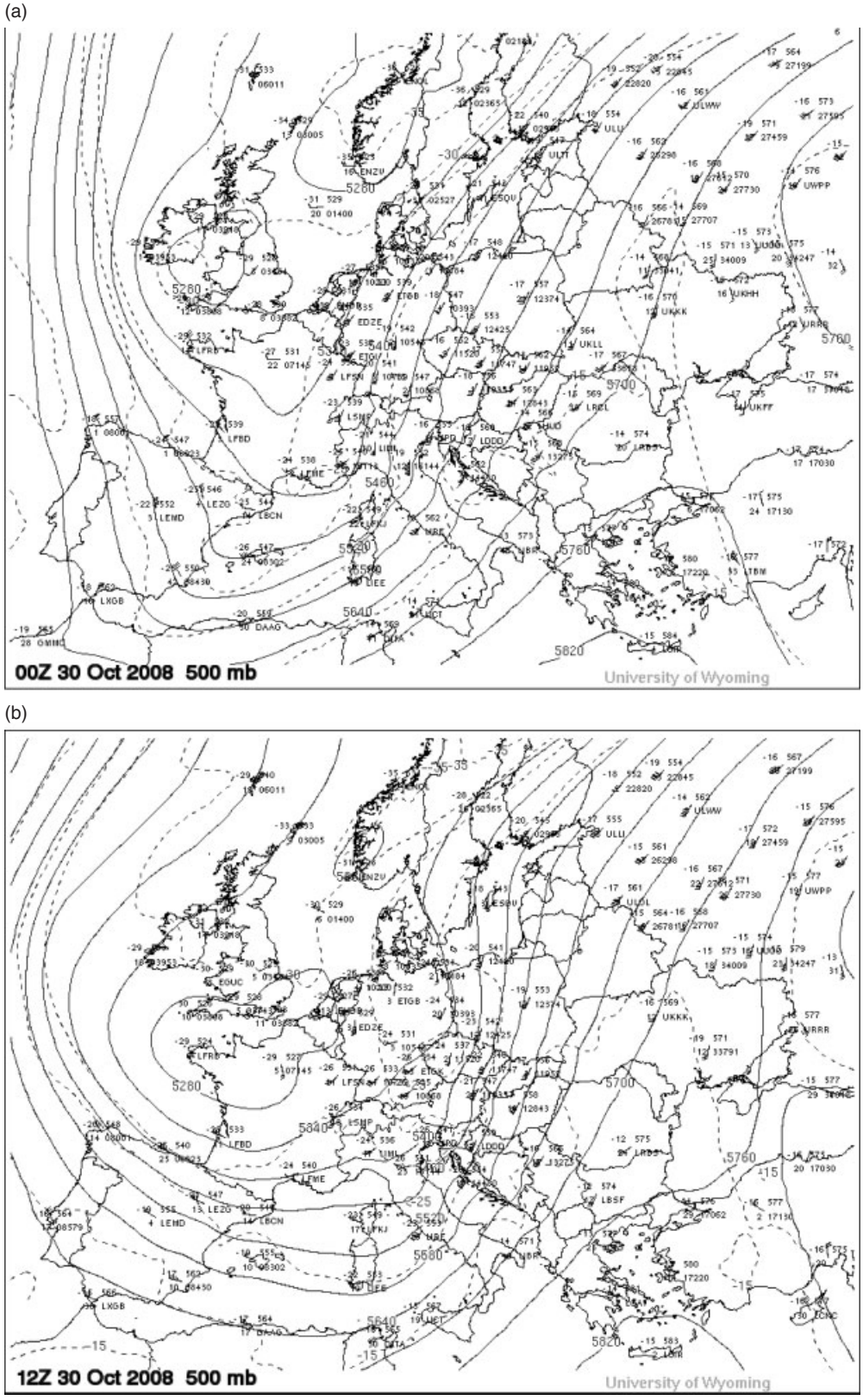

Figure 4. 500 hPa geopotential height field and temperatures at 0000 UTC (a) and 1200 UTC (b) 30 October 2008. Height contours are drawn at 60 m intervals. Courtesy University of Wyoming.

UTC a relatively dry region was present to the west of Ireland, extending southwards and eastwards as far as the western English Channel, Cornwall and southwest Wales. Deeper moisture was visible to the east, over much of Wales and the western half of England, in the vicinity of the surface occlusion. The sequence of satellite images suggests that the positive vorticity anomaly associated with the dry region was advected cyclonically

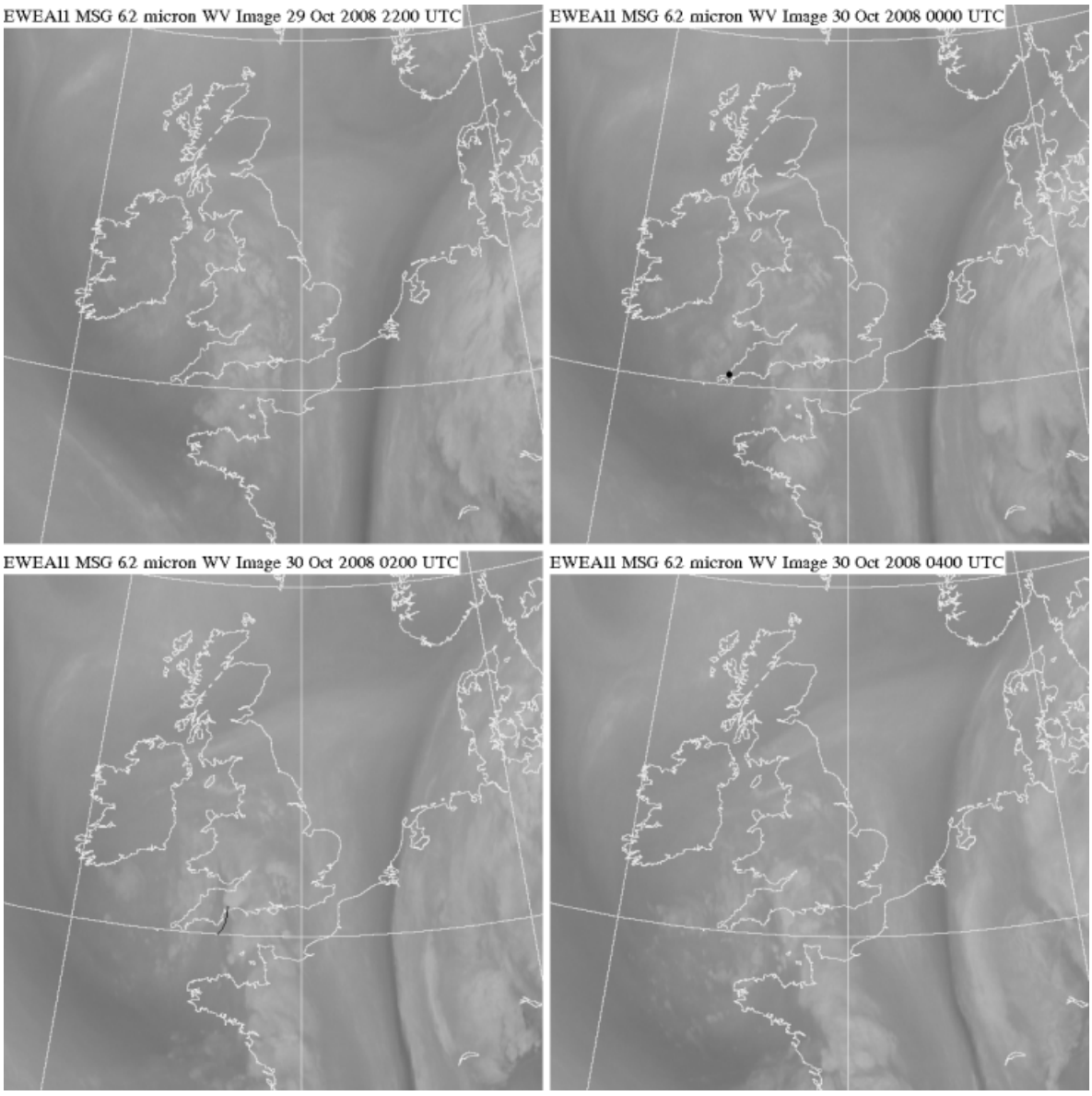

Figure 5. METEOSAT Second Generation (MSG) water vapour channel (6.2 μm) satellite images over the United Kingdom and northwest Europe. Data are shown at 2 h intervals between 2200 UTC 29 October and 0400 UTC 30 October 2008. Black dot in the 0000 UTC image denotes the location of Camborne. Curved line in the 0200 UTC image marks the western edge of the low level moisture plume. (Copyright EUMETNET and Met Office (2009)).

around the height minimum between 2200 UTC 29 and 0400 UTC 30 October, over southwest England and the western English Channel. The sequence of images also reveals divergent flow in this region: small scale brightness temperature variations reveal flow towards the east or northeast over southwest England and south Wales, and towards the southeast over north-western France. The approaching vorticity anomaly and upper level divergent flow, and their associated forcing for ascent, are likely to have contributed to destabilization over southwest England. In fact, the rapid development of deep convection over the area is visible in the satellite water vapour imagery, owing to the moisture associated with the developing anvil shields of the convection. This can be seen, for example, over south Devon by 2330 UTC and over east Devon and much of Somerset by 0200 UTC. The extensive, near-circular anvil shield visible at the latter time was associated with the convective system responsible for the Ottery St Mary flood. Cloud-top height satellite products revealed that the convective tops extended to around 8 km above ground level (AGL). The sequence of images shows that the storm developed along the eastern edge of the dry upper level air and associated positive potential vorticity anomaly.

One consequence of the slow movement of the occlusion over Devon is that the forcing for ascent and resulting destabilization ahead of the positive potential vorticity anomaly overran part of the stalling portion of the occlusion. This can be seen by comparing the locations of the rear edge of the occlusion rain band and leading edge of the dry region at hourly intervals between 2100 UTC on 29 October and 0200 UTC on 30 October (the

solid line in Figure 5 shows the location of part of the surface occlusion over east Devon and Lyme Bay at 0200 UTC on the corresponding satellite water vapour channel image). This may explain the observed rapid increase in convection along the rear edge of the rain band after 2200 UTC. As will be shown in the following section, mesoscale variations in surface wind and dew point temperatures also acted to focus the developing convection on a smaller scale into preferred locations along the rear edge of the occlusion.

Figure 6 is a tephigram constructed using the 0000 UTC radiosonde data from Camborne, Cornwall. At this time, Camborne was located on the southern edge of the 500 hPa height minimum and cold pool, and within the dry region visible in vapour imagery (Camborne's location is marked in the 0000 UTC panel of Figure 5). The dry air is clearly evident at all levels above 800 hPa. Below 800 hPa, the air is somewhat moister, though still sub-saturated. The temperature lapse rate was particularly steep (approaching dry adiabatic) in two layers: the lower from 900 to 800 hPa and the upper layer from 650 to 550 hPa. A small amount of convective available potential energy (CAPE) was present in the Camborne profile, of 46.6 J kg^{-1}. However, when the tephigram is modified using surface temperature and dew point temperature as observed at Sidmouth at 0100 UTC, corresponding to the storm inflow region at this time, a considerably larger CAPE of 204 J kg^{-1} results. It should be noted that this value is well within the range of CAPE typically observed in association with UK thunderstorms in the warm season, and it is not unusual even in the cool season in coastal regions.

5. Mesoanalysis

Hourly mesoanalyses of surface wind speed, wind direction, mean sea level pressure and dew point temperature were constructed using available surface observations, for the period 1800 UTC 29 to 0400 UTC 30 October 2008. Figure 7 shows analyses at intervals of 2 h through this period. At 1800 UTC, a sharp surface pressure trough lay to the west of southwest England and Wales, extending to the south of the surface depression centre which was at this time centred close to northwest Ireland. Relatively high dew point temperatures ($>7\,^{\circ}$C) are evident over sea areas to the west of Wales and southwest England, with the axis of highest dew point temperatures broadly collocated with that of the surface pressure trough. Dew point temperatures approaching 10 °C, located southwest of Cornwall, appear to have been associated with the tip of the occluding warm sector. The trough moved east and sharpened in the following 2 h, the trough axis having reached central Cornwall and the far southwest of Wales by 2000 UTC. At 1800 and 2000 UTC, surface wind observations reveal significant convergence along the axis of the trough, with south to southeasterly winds present east of the trough and northwesterly winds to the west. Comparison with radar rainfall imagery shows that the trough axis and associated convergent wind shift line was located close to the rear edge of the occlusion rain band. The mesoanalyses suggest that trough disruption commenced some time after 1800 UTC, with evidence of a small 'cut off' low pressure centre having formed over Cornwall, close to the base of the trough by 2000 UTC. This small depression appears to have been no larger than 30 or 40 km in diameter and will subsequently be referred

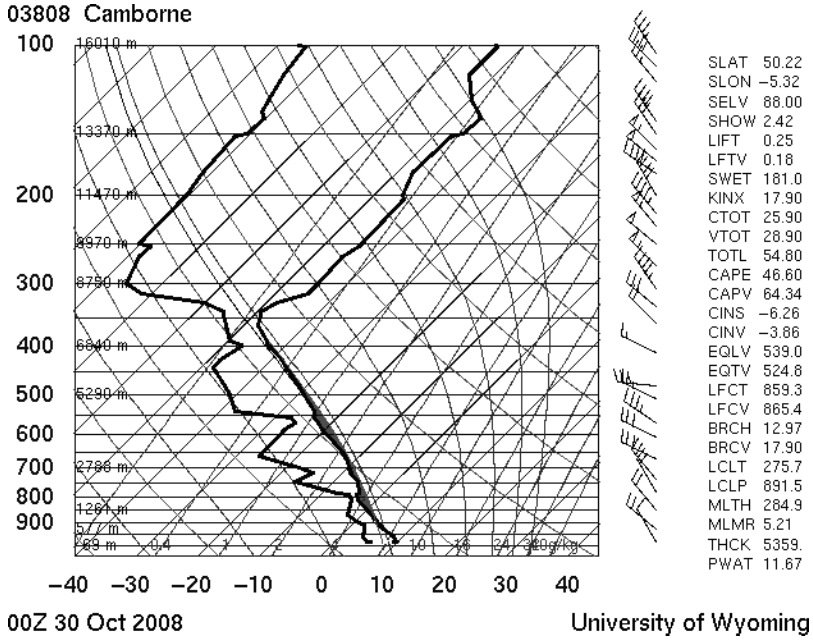

Figure 6. Tephigram constructed from 0000 UTC 30 October 2008 Camborne radiosonde data. Right and left-hand bold lines show temperature and dew point temperature, respectively. Wind profile is shown by barbs on right hand side. Shaded area shows CAPE obtained using observed surface temperature and dew point temperature in the storm inflow. Pressure and temperatures are in hectopascals and degrees Centigrade, respectively. Courtesy University of Wyoming.

to as a 'mesolow'. It is interesting to note that the sharpening and eventual disruption of the trough occurred close to the time that the left exit region of the 500 hPa jet, moving southward as previously discussed, approached closest to the surface trough axis during the early evening hours. This process may therefore have resulted from locally enhanced surface pressure falls induced underneath or close to the jet exit.

During the following few hours the larger, synoptic scale depression continued to edge south over the Irish Sea area towards southwest England. Meanwhile, the mesolow deepened substantially, moving slowly eastwards along the southern flank of the synoptic-scale low pressure centre. By 2200 UTC the feature was located in the vicinity of Plymouth. It continued to move eastwards over the following 2 h, being located by 0000 UTC 30 October in the vicinity of Torbay. Although pressure within the larger low pressure centre fell steadily through the analysis period, central pressure within the mesolow fell more rapidly, by approximately 1.5 hPa *per* hour between 2200 and 0200 UTC. As a result, a significant cyclonic surface flow had developed in association with the mesolow by 0000 UTC, as revealed by surface wind observations. This cyclonic circulation was also revealed by Doppler radar radial winds from about 0100 UTC (not shown): inbound and outbound radial velocities exceeding 15 m s^{-1} were observed on the east and west flanks of the mesolow, at the radar beam height of approximately 0.5 km (at this range). From 0000 UTC, the mesolow started to move in a more northeasterly direction, though at decreasing speed, approximately following the south Devon coastline. By 0100 UTC the mesolow was centred near the approaches to the Exe Estuary, and by 0200 UTC the feature had approached the Ottery St Mary area. Pressure gradients appear to have been particularly steep on the northeast flank of the mesolow from 0000 UTC: surface observations accordingly show moderately strong and increasing southeasterly flow over east Devon as the feature approached. Surface observations from privately owned weather stations in Sidmouth and Feniton, and also from the Met Office station at Dunkeswell, showed a general backing of the wind direction between 2300 and 0100 UTC, from southerly to southeasterly.

The surface dew point temperature analyses in Figure 7 reveals that as the mesolow deepened the previously rather broad region of higher dew point temperatures located in the vicinity of the trough progressively narrowed into a north-south orientated plume, located south and east of the mesolow. This feature moved slowly eastwards and slightly northwards over the analysis period, in conjunction with the movement of the mesolow. The thunderstorms over east Devon appear to have occurred close to the northern tip of this moist plume from about 0000 UTC. Near the south coast of east Devon, dew point temperatures reached between 7 and 8 °C (7.4 °C in Exeter at 2320 UTC and 7.8 °C in Sidmouth at 0200 UTC) as the plume approached. However, these relatively high dew point temperatures made little progress inland over Devon: the highest observed dew point temperature at Dunkeswell over the analysis period was just 5.5 °C, and at Liscombe, 4.5 °C. The sharpening of dew point temperature gradients at the northern edge of the moist plume and continued advection of moisture northward along the eastern flank of the mesolow suggest that strong low-level moisture convergence was occurring close to the tip of the plume, immediately northeast of the mesolow. The surface wind observations are also highly suggestive of localized strong convergence in this area. Stations to the north and west of the storm reported generally northerly winds at 0200 UTC (e.g. a 5 knot northerly and a 5 knot northeasterly at Exeter and Feniton, respectively), with simultaneous observations of stronger, southeasterly winds on the opposite side of the storm system less than 20 km away (e.g. a southeasterly wind of 10 gusting 27 knots at Sidmouth).

After 0300 UTC, the analyses suggest that the mesolow began to fill somewhat, at least relative to the 'background' pressure field in the centre of the larger scale depression, which continued to fall slowly. By 0400 UTC the feature had apparently largely dissipated. Broad-scale southeasterly or easterly flow associated with the pressure gradient on the northern flank of the synoptic-scale depression had begun to influence much of Devon by this time, as the larger scale depression centre started to slip away to the south of the area. This appears to have resulted in advection of drier air from the east, resulting in a gradual decrease of the dew point temperatures over much of east Devon, as the moistest air associated with the dew point plume gradually became restricted to adjacent parts of the English Channel.

It can be seen from Figure 7 that the development of the surface moist plume, deepening of the mesolow and the associated increase in low-level convergence were observed for a number of hours prior to commencement of the storm over east Devon. This suggests that careful monitoring of the surface observations may have allowed successful identification of a smaller area, of order 20–30 km in scale, which was likely to be particularly prone to persistent and vigorous convection, within the broader region experiencing a general trend for increased instability. Although the available surface synoptic stations struggled to resolve the mesolow (the scale of the latter being approximately the same as the average spacing between surface stations) the Doppler radar radial wind observations added value in this situation: not only was the mesolow clearly resolved, but also the increase in low level circulation associated with the mesolow, the increasing convergence, and the gradual reduction in its translational speed, were revealed. Therefore, 'rapid-update' analysis of all available surface observations (ideally frequency better than once *per* hour) and simultaneous monitoring of complementary data such as the Doppler radial wind data is to be recommended in similar situations, especially when high resolution models have already identified a risk of large rainfall totals. Although somewhat specific to this event,

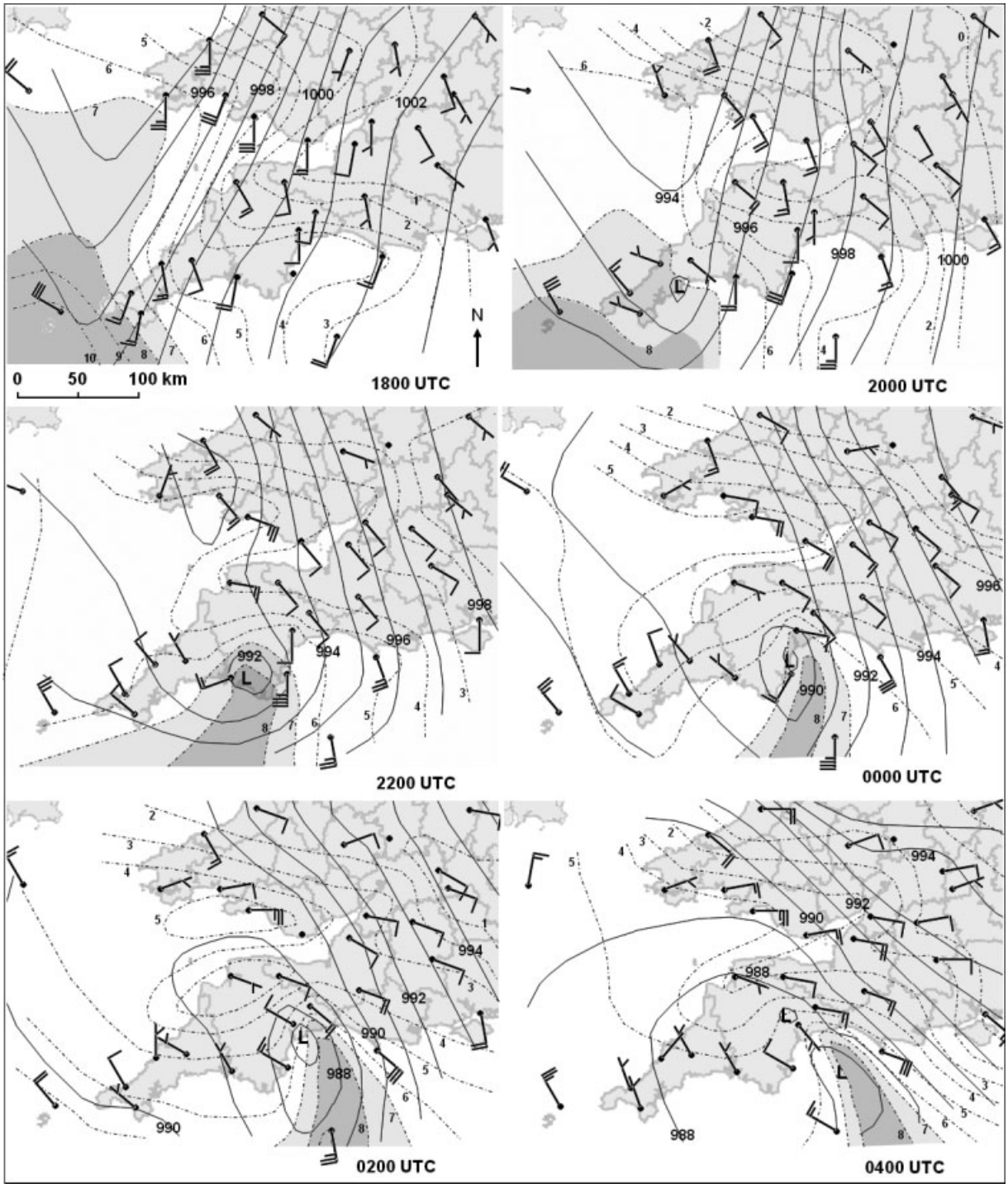

Figure 7. Sequence of surface mesoanalyses showing mean sea level pressure field (isobars drawn as solid lines at 1 hPa intervals), surface wind speed and direction (wind barbs) and dew point temperature field (isodrosotherms drawn as dashed lines at 1 °C intervals) over southwestern parts of the United Kingdom for the period 1800 UTC 29 October to 0400 UTC 30 October 2008. Light and heavy shading highlight areas with dew point temperature of >7 and >8 °C, respectively.

this approach would also prove beneficial in many convective situations, since the occurrence and location of convection is often highly sensitive to factors such as the magnitude and persistence of surface convergence, and small variations in surface temperature or dew point temperature. Of course, the utility of each of the different types of observations would vary from case to case. However, this event demonstrates that simultaneous analysis of several different observations types can provide much more insight than analysis of fewer observation types in isolation.

6. Radar data

High resolution radar reflectivity data from the Met Office's Cobbacombe radar has allowed detailed analysis

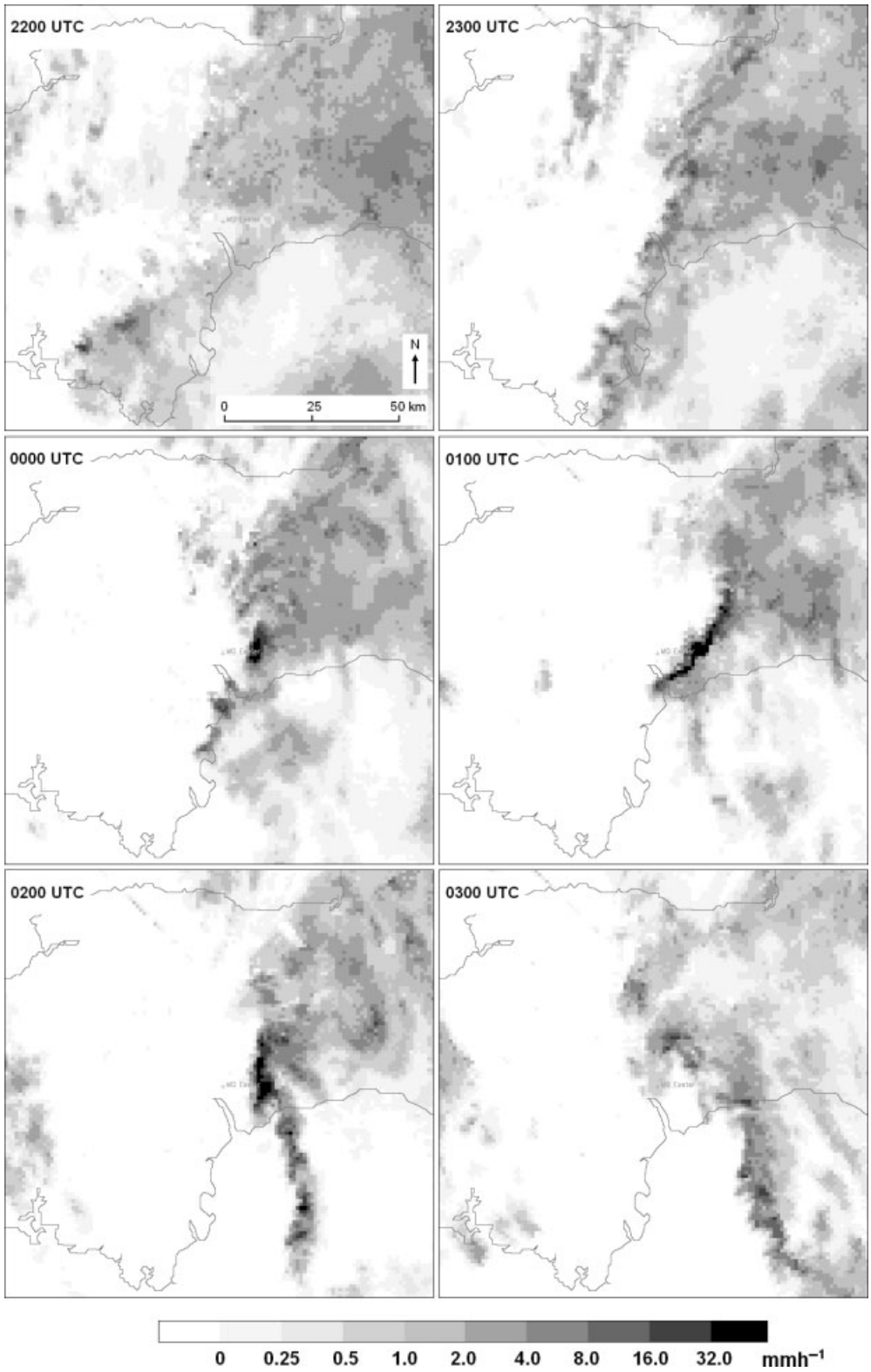

Figure 8. Sequence of 1 km resolution instantaneous rainfall rate (millimetres per hour) over southwest England, derived from the Met Office Cobbacombe radar reflectivity data. Data are shown at hourly intervals over the period 2200 UTC 29 October to 0300 UTC 30 October 2008. Area shown has width of approximately 110 km. (Crown Copyright Met Office (2009)).

of the development and evolution of the east Devon convective system. Figure 8 shows a sequence of 1 km resolution instantaneous rainfall intensity images, which are routinely generated from the raw radar reflectivity data. At 2200 UTC, areas of light to moderately heavy 'stratiform' precipitation were present over much of the eastern and southern portions of southwest England and adjacent waters. This rainfall area formed part of the weakening rain band associated with the surface occlusion which moved east across the area during the evening

of the 29 October before becoming slow moving. Slight orographic modification of rainfall rates is suggested by the areal distribution of rainfall rates at this time, with heavier precipitation located close to windward (south facing) coasts and over higher ground such as the Blackdown Hills, including the area just south of Ottery St Mary. The surface pressure trough and associated convergent wind shift line were located close to the western edge of this rain band as previously discussed: Doppler radial velocity data (not shown) also revealed a persistent, steep gradient in radial winds close to the rear edge of the occlusion rain band through much of the analysis period, indicative of the sharp wind shift line collocated with the trough axis. This wind shift line passed Exeter between 2300 and 2340 UTC, during which time the wind veered abruptly from southerly to northwesterly. West of this line, conditions were much drier, though with scattered convection affecting northwest Devon.

The heavier cells over south Devon at 2200 UTC, close to the rear edge of the occlusion rain band, indicate the location of the developing mesolow at this time. When viewed in a sequence, 5 min frequency rainfall intensity images clearly show cyclonic rotation of the cluster of cells around the apparent mesolow centre. The location of the mesolow centre, as could best be estimated from the surface pressure mesoanalyses, was congruent with that of the rotation observed in radar data. For this reason, the location of the mesolow centre in the mesoanalyses was 'fine tuned' using the radar data from 2200 UTC onwards. From 0100 UTC, the centre of the mesolow could also be determined from the Doppler radial wind pattern as mentioned previously: again, the positioning of the low was clearly in agreement with that inferred from the surface pressure mesoanalyses and the radar rainfall intensity sequence. The radar reflectivity data provides some confirmation of the increased potential for persistent convection in the vicinity of the mesolow, which was inferred from the analysis of surface observations. In a real-time situation, the observed persistence of convection at this time might have increased confidence that large rainfall totals would occur in association with the feature at some stage. Once identified, a trend for increasing risk of large rainfall totals may have been identified in real time as the translational speed of the mesolow reduced, and as the feature continued to deepen, in the subsequent 1–2 h.

Between 2200 and 2300 UTC the rear edge of the occlusion rain band moved only very slowly eastwards, being located by 2300 UTC in a line running from south Devon, through the Exeter area and towards the Somerset coastline. Reflectivity gradients along the western edge of the rain band sharpened over this hour, with slightly heavier cells having developed at several locations close to the edge of the rain band by 2300 UTC. A very rapid increase in convective activity occurred between 2315 and 2330 UTC, as shown by the development of echoes with rainfall rates exceeding 32 mm h^{-1}. The strongest convection developed along a small section of the rear edge of the rain band, extending from the location of the mesolow north-eastwards for a distance of about 50 km. During the following 30 min convection continued to increase in coverage and intensity over the same area as the mesolow moved slowly northeast, parallel to the rear edge of the rain band. By 0000 UTC the most intense convective cell was located approximately 15 km east of Exeter, over the Ottery St Mary area. By 0100 UTC, a solid line of intense convective cells stretched northeast from the mesolow centre, now located over the Exe Estuary, northeast through the Ottery St Mary area and towards Dunkeswell. Whilst the rainfall intensity images show a near-continuous line of intense rainfall rates (>32 mm h^{-1}), the 5 min sequences of raw reflectivity data (not shown) reveal movement of embedded precipitation cores northeastwards along the line. This motion can be attributed to the mean flow in the convective layer, as will be shown subsequently. Radar data show the repeated development of new convective cells close to the southwest end of the line, just northeast of the centre of the mesolow and very close to the northern tip of the surface dew point plume, as identified by the surface mesoanalysis at this time. As a result, the motion of the convective system as a whole was negligible.

The convective system remained in this quasi-steady state for at least an hour, until around 0130 UTC, though the orientation of the long axis of the convective system slowly changed from northeast-southwest towards a more north-south direction (this was at least in part related to a gradual change in the convective layer mean wind, as will be shown subsequently). Very high rainfall rates occurred continuously along the length of the convective system through this period. After 0130 UTC, the mesolow appears to have moved north-northeast along the long axis of the convective system, resulting in rather marked cyclonic rotation of the system as a whole for a time (again, this is best observed when viewing the 5 min sequence of radar reflectivity imagery). Since the centre of rotation was by this time located close to Ottery St Mary, the locations previously affected by the heaviest rainfall continued to be affected for a while longer. After 0200 UTC, the area of most intense convection, having advected with the cyclonic low level flow around towards the northern flank of the mesolow, started to move steadily towards the northwest, weakening rapidly in the process. At about the same time a line of strong convective activity developed along the southern flank of the mesolow, coincident with the axis of the sharp surface pressure trough, extending southward into the English Channel. During this period, the convective system over east Devon rapidly lost its linear structure. Peak rainfall rates decreased to below 32 mm h^{-1} by 0230 UTC, and thereafter the remnants of the system continued to move northwestwards under the influence of increasing broad-scale southeasterly flow, expanding and weakening further in the process.

Precipitation intensity was undoubtedly very high on this occasion, as revealed by eyewitness accounts of the storm, rain gauge data and radar reflectivity values. Peak

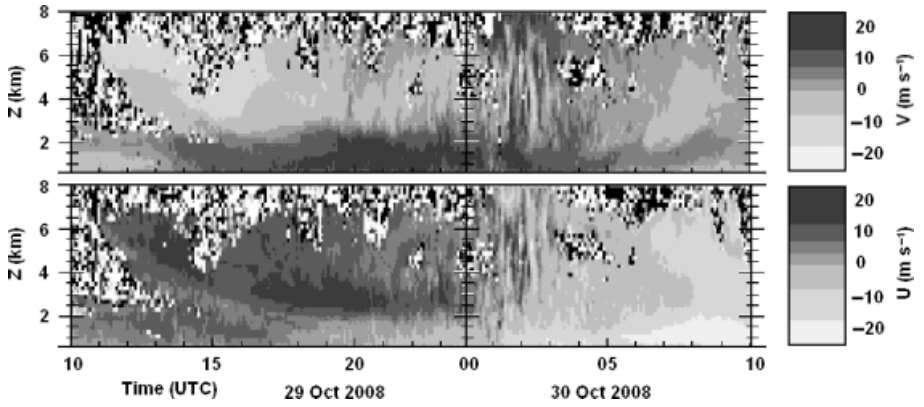

Figure 9. Time-height plot of u and v wind components, as observed by the Met Office Dunkeswell wind profiler, for the 24 h period ending 1000 UTC 30 October 2008.

reflectivity values in the core of the convective system were persistently in the range 48 ± 4 dBZ between 0000 and 0200 UTC, with the area of reflectivities in this range exceeding 20 km in length at times. Although these reflectivity values are close to the upper limit of values observed in association with thunderstorms in the United Kingdom, they are apparently not exceptional: reflectivities exceeding 56 dBZ are typically observed on several occasions each year over the United Kingdom, in association with the cores of thunderstorms, usually in the warm half of the year. However, on most of these occasions, the convective cores move at considerable speed so that the highest reflectivity values affect given locations only for very short periods of time, of order 5–10 min. It is the sustained occurrence in this case of very high reflectivity values over the same area, for a period of over 2 h, which is highly unusual. The product of precipitation duration and intensity was therefore undoubtedly exceptional over a small area in this case, as is confirmed by the estimated rainfall totals and the nature of the damage which occurred.

7. Wind profiler data

Figure 9 shows a time-height plot of the u (zonal, westerly flow positive) and v (meridional, southerly flow positive) components of wind obtained from the Met Office Dunkeswell wind profiler for the 24 h period ending 1000 UTC 30 October 2008. The plots show data from approximately 0.5 km to a maximum of 8.0 km AGL. At the broadest level, the plots reveal two distinct wind flows in the vertical, the interface between these marked by a well-defined shallow layer of strong wind shear. The first, low-level flow extended from the ground to approximately 2.5 km AGL. Within this layer, v flow was relatively constant at approximately 10–15 m s^{-1} over the primary period of interest (2100 UTC 29 to 0400 UTC 30 October). The u component of flow was close to zero at 2100 UTC, but decreased steadily thereafter, with values of approximately −10 to −15 m s^{-1} by 0300 UTC. Therefore, the winds in this layer were initially approximately southerly, but backed southeasterly and increased in magnitude with time. The flow in this layer is clearly consistent with surface wind observations to the south and east of the wind shift line along the rear edge of the occlusion rain band, and specifically to the east and northeast of the approaching mesolow, as might be expected when comparing the location of Dunkeswell and that of the surface pressure trough and mesolow as shown by the surface mesoanalyses. It should be noted that the pressure trough axis and surface wind shift line never quite reached Dunkeswell, and as a result the wind profile on the northwestern side of the occlusion and surface trough was not sampled by this profiler. It is interesting that the observed backing and strengthening of the flow between 0000 and 0300 UTC within the surface to 2.5 km AGL layer was at a maximum at low levels, with the u component of flow reaching −20 knots or less at heights below 1.0 km AGL. This suggests that the mesolow and its associated cyclonic flow was a relatively shallow feature, decreasing in intensity with height.

The second flow extended from 2.5 km to at least 7 km AGL, and was characterized by near zero v component of flow throughout the period of interest. The u component in this layer shows a reversal through the same period, with initially positive values of 10–15 m s^{-1} decreasing steadily to weakly negative values (around −5 m s^{-1} by 0300 UTC). This flow is consistent with the circulation around the larger, synoptic scale geopotential height minimum at mid- and upper-levels, as it slipped south over the area: early in the period westerly flow was observed when the height minimum was located to the north and northwest, but the flow dropped out as the centre moved close by, followed by increasing easterly flow as the centre of the height minimum moved to the south. Note that there is no indication of a southeasterly flow which might be expected on the northeast flank of the mesolow within this layer, again suggesting that the mesolow was a shallow, surface based feature which did not extend into middle and upper levels of the troposphere.

These two basic flow regimes were by no means restricted to the area close to Ottery St Mary. For example, the Camborne wind profiler measurements

show a similar pre-frontal wind structure (the surface occlusion and wind shift passed Camborne at 1800 UTC 29 October). South to southwesterly flow up to about 2.0 km AGL is evident, with northwesterly winds above. In the post frontal regime, the Camborne wind profiler shows rather uniform, light to moderate northwesterly flow, extending from the surface to at least 7 or 8 km AGL (this is also shown by the 0000 UTC 30 October Camborne tephigram, see Figure 6). This further illustrates the significant convergence which existed along the trough axis at low levels, and shows that this convergence extended to approximately 2 or 2.5 km AGL (i.e. over the same layer in which winds with a southerly component were observed east of the surface front). The effect of the mesolow would have been to increase the convergence present along the trough axis and rear edge of the occlusion rain band locally, owing to a backing and increase in speed of the pre-frontal low level flow to its northeast and east.

8. Discussion

The observations presented herein provide a number of clues as to how such intense convection was able to persist over a small area for such an extended period of time. Perhaps of most importance is the link between the location of convection and that of the mesolow. As noted previously, the most intense and sustained convective activity occurred immediately to the northeast of the mesolow centre, where convergence, warm advection and moisture advection appear to have been maximized, and very significant. Since the mesolow only moved very slowly by the time it reached east Devon, the location of maximum low level convergence and moisture convergence remained almost stationary for at least 2 h from around 0000 UTC, and, therefore, the area in which new convection was triggered also remained essentially stationary. The mean convective layer winds were parallel to the low level convergence axis during this period: consequently, the residence time of convective cells over the convergence line was maximized. Whilst some convection had occurred in association with the mesolow from 2230 UTC, the intensity of the convective cells only increased markedly as the mesolow moved northeast from Torbay after 2330 UTC. This may have been partly because of a trend of upper level cooling and destabilization associated with the approach of the 500 hPa cold pool. However, more important is probably the observed trend for increasing low level cyclonic flow around the mesolow as it continued to deepen, and resulting increased low level convergence on its northeast flank. Once deep convection had become established, low level convergence would likely have been focussed even more strongly by the storm outflow into a narrow band along the southeastern flank of the storm system, owing to the large vector difference between the observed cell motion (towards the northeast) and the low level southeasterly winds. The relatively dry environment would be favourable for development of a significant cold pool, which may have further enhanced low level ascent by undercutting the impinging warmer, moist inflow air.

The Camborne tephigram (Figure 6) shows that the precipitable water (PW) values were low, at just 11.7 mm. Modifying the Camborne sounding by taking into account the observed surface dew point temperature, and assuming a saturated inflow layer 2.0 km deep, gives a slightly higher value of 12.9 mm. As has previously been mentioned, flash flood events in the United Kingdom and elsewhere globally are typically associated with significantly higher values of PW (e.g. Maddox *et al.*, 1978, 1980; Golding *et al.*, 2007): even considering the effect of increased moisture at low levels close to the storm, the PW value in the storm environment on this occasion was anomalously low. The observed surface dew point temperature in the storm inflow ($\sim$8 °C) was also low compared to other flash flood events in the United Kingdom.

It is interesting to consider how the observed peak rainfall rates, which were of order 100–150 mm h^{-1}, could have occurred in such an environment. The observed CAPE of $\sim$200 J kg^{-1} implies a maximum updraft speed of 20 m s^{-1}. In practice, a better estimate of updraft speed is half this value, i.e. 10 m s^{-1}, owing to the effects of precipitation loading and entrainment on the parcel buoyancy. Note that this is the updraft speed at the top of the convective layer, after the parcel has accelerated though the whole CAPE layer. Assuming an even distribution of CAPE through this layer, and that the parcel starts at rest at the level of free convection (LFC), the average updraft speed over the convective layer would be around 5 m s^{-1}. However, the tephigram suggests that CAPE was on this occasion concentrated to some extent at lower levels, which would result in stronger parcel accelerations at low levels and a greater mean updraft speed over the convective layer, compared to a situation in which the CAPE was distributed evenly over the layer. Calculations made using the observed CAPE profile result in a larger mean updraft speed of 8.5 m s^{-1}.

Estimations of the updraft speed required to sustain the observed rainfall rates may be made using the modified Camborne tephigram. Storm totals of 200 mm suggest a mean rainfall rate over the 3 h period ending 0300 UTC of 67 mm h^{-1}. For the purpose of calculating required updraft speed, it is assumed that the 12.9 mm precipitable water given by the modified tephigram is contained entirely within the 0–2 km AGL inflow layer. Further, it is assumed that as this layer ascends to the top of the storm (i.e. to 6–8 km AGL), all water is condensed out, and that all condensed water falls to ground as precipitation (i.e. storm precipitation efficiency of 100%). Under these circumstances, a precipitation rate of 67 mm h^{-1} would require a mean updraft speed of 8.7 m s^{-1}, and the most conservative value of estimated peak rainfall rate, of around 100 mm h^{-1}, would require a mean updraft speed of 12.9 m s^{-1}. In practice, these are minimum required updraft values, since the storm's

precipitation efficiency would almost certainly be less than 100%. Comparison with the estimates of updraft speed resulting from the CAPE in the storm environment clearly shows that the mean rainfall rate, and certainly the peak rates, cannot be explained by the magnitude of updrafts resulting from parcel buoyancy alone.

The most likely explanation is that updraft speed was enhanced by the low level convergence on this occasion, as has previously been suggested. Resulting ascent forced by this convergence would ensure that parcels would have acquired significant ascent rates by the time they reached the LFC. At around 0100 UTC, surface observations reveal a wind difference of 7.5 m s^{-1} in the line-normal direction, across the convergence line collocated with the storm. As has been mentioned, wind profiler data reveals that the convergence layer was around 2–2.5 km deep (note however that the convergence magnitude probably decreased somewhat with height over this layer). If it is assumed that the convergence line was of order 2 km wide (this agrees with the observed width of the intense convective line, and also that of convergence lines more generally), the resulting ascent may be estimated by applying the continuity equation. If it is assumed that there was no line-parallel divergence, and taking the convergence line depth as 2.25 km, the resulting updraft strength at the top of the convergence layer would be approximately 8.4 m s^{-1}. Adding this to the buoyancy-derived mean updraft of 8.5 m s^{-1} gives a combined updraft speed of $\sim$17 m s^{-1}. This updraft speed could explain the observed peak rainfall rates, e.g. the required minimum of 12.9 m s^{-1} for 100 mm h^{-1} rates, as calculated previously. These results suggest that strong low-level convergence was a significant factor in the generation of high rainfall rates in this case, with the magnitude of ascent resulting from convergence likely comparable to that associated with parcel buoyancy. The forced ascent and continued moisture convergence allowed precipitation rates to become much higher than might typically be observed in environments with similar values of PW. This demonstrates that when predicting the risk of exceptional convective events, the use of PW or other moisture-related parameters in isolation can be misleading, particularly in situations when other favourable factors (such as surface convergence) may compensate for values which are seemingly unsupportive of such events.

Another probable source of low-level ascent in this case is orographic uplift. Southeasterly inflow on the northeast flank of the mesolow would have experienced some mechanically forced ascent as it encountered the low ridge of southwest to northeast orientated hills, located just north of the coastline and extending from near Exmouth towards Ottery St Mary. It is difficult to provide any direct evidence that this process occurred at the time of the Ottery St Mary storm, though rainfall rates in the occlusion rain band on the evening of 29 October were observed to have been a little higher just north of the east Devon coast, illustrating that weak orographic forcing for ascent was occurring at that time in the same locality, with a similar surface wind direction. An orographic contribution to low-level ascent could also explain why the earlier convection associated with the mesolow increased temporarily in intensity as the feature moved over higher ground in south Devon, and decreased again as the mesolow approached Torbay. Given typical gradients near West Hill of 100 m 3 km^{-1} in the direction parallel to the storm inflow, and an observed surface inflow of 5 m s^{-1}, implied ascent rates are on the order of 0.2 m s^{-1}. On balance then, it appears that the flow field around the mesolow, and its induced low-level convergence, was the dominant factor in determining the exact location of the most persistent convection, whilst the orographic effects were of secondary importance.

The initial trough disruption and development of the mesolow can perhaps most likely be attributed to forcing associated with the left exit of the upper level jet, as previously discussed. Subsequent deepening may be attributed to forcing associated with continued vorticity advection aloft (indicated by the approach of the dark region in satellite WV imagery, see Figure 5). However, it could equally be speculated that the deepening was attributable to the effects of latent heat release in mid-levels associated with the persistent convection. Weak mid- and upper-level winds meant that cells did not move far from their initiation point allowing such effects to operate for a relatively long period close to the mesolow. This effect would also be maximized where convection was most intense and persistent, i.e. immediately north-east of the mesolow. This may explain the eventual movement of the centre of the mesolow northeast through the pre-existing convective line. It could also explain why the mesolow remained a relatively shallow, surface-based feature.

One interesting feature revealed by sequences of radar rainfall intensity data is the cyclonic rotation exhibited by the convective system as a whole between 0100 and 0230 UTC. The rotation was slow at first, only observable as a very gradual change in the orientation of the long axis of the convective system. However, rotation became increasingly rapid after 0130 UTC as the centre of the mesolow moved north-northeastwards through the convective system. Given that convective cell motion can usually be approximated by the mean wind in the convective layer (e.g. Corfidi, 2003), it is perhaps not surprising that the cell motion within the system became increasingly dominated by the low level cyclonic flow pattern, as low level winds strengthened and upper level winds weakened (as shown by the Dunkeswell wind profiler observations: see Figure 9). To investigate further the relationship between the convective layer mean wind and cell motion on this occasion, a mean convective layer wind was calculated from wind profiler data for each hour between 0000 and 0300 UTC 30 October, and compared with the observed cell motion at each hour. The cell motion vector on the flank of the storm system corresponding to the location of the wind profiler (northeast then east) was used. This was estimated from the motion of individual convective

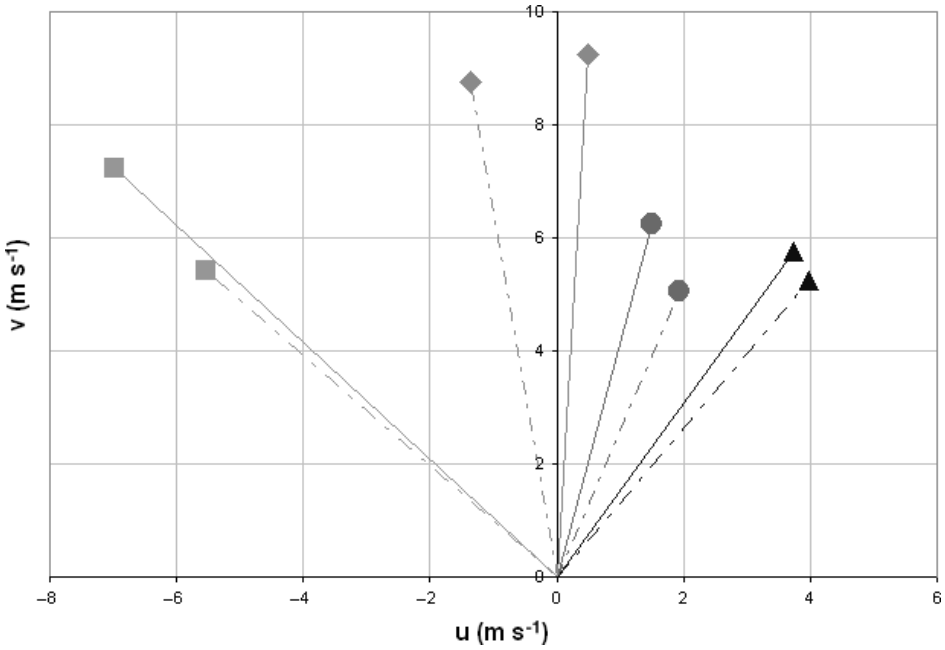

Figure 10. Observed cell motion vectors (dashed lines) and convective layer mean wind vectors (solid lines) for each hour in the period 0000 to 0300 UTC 30 October 2008. Mean 0000 UTC Mean 0100 UTC Mean 0200 UTC Mean 0300 UTC Storm 0000 UTC Storm 0100 UTC Storm 0200 UTC Storm 0300 UTC.

cells or embedded convective elements using the 5 min sequences of radar reflectivity data. The convective layer mean wind was calculated following the method of Corfidi *et al.* (1996), in which an average of the wind speed at four representative levels is calculated. However, the levels chosen were re-scaled to reflect the relatively small depth of the storm on this occasion (a scaling factor of 2/3 was applied to the levels used by Corfidi *et al.* (1996), since the storm depth here was 8 km, as compared to 12 km as typically seen in the United States in the warm season).

Figure 10 shows the observed cell motion and predicted (convective layer mean) motions calculated in this way, for each hour between 0000 and 0300 UTC. The convective layer mean wind was observed to back and increase through the period. The evolution of the mean wind is closely reflected by the evolution of cell motion, which also shows a backing and increase in magnitude over the analysis period. This demonstrates that the cells moved approximately with the mean wind on this occasion, and that the time variation in cell motion was likely a result of changes in the convective layer mean wind, at least close to the location of the wind profiler. It must be emphasized that the cyclonic rotation exhibited by the storm system should not be confused with rotation exhibited by supercells. The latter is attributable to tilting by the storm updraft into the vertical of strong horizontal vorticity present in environments of substantial vertical wind shear (Rotunno, 1981). Rotation in this case occurred as a consequence of the influence on cell motion of a cyclonic low-level flow pattern, associated with the pre-existing mesolow, under conditions of relatively weak mid- and upper-level winds. Furthermore, the observed area of rotation in this case was significantly larger in diameter than is typically observed for supercell mesocyclones, the latter being generally around 2–10 km in diameter.

The combined effect of cyclonic low level flow around the mesolow and an increasing easterly component in the middle and upper level winds resulted in increasingly rapid movement of the core of the convective system towards the northwest after 0200 UTC, which eventually led to the storm's demise. As the cells gained a northwestward motion, low level inflow and convergence would have been reduced, since the component of cell motion directed opposite to that of the low level inflow was significantly reduced (although the increasing magnitude of the low level south-easterly flow would have perhaps compensated for this initially). This probably explains the weakening of the tight reflectivity gradients which had previously been present on the southeast flank of the storm; the storm apparently 'expanded outwards' (i.e. increased in overall width) as it dissipated. As the centre of the system moved northwestwards, it also became increasingly displaced from the low level moisture plume, which likely reduced the dew point and effective CAPE of the storm inflow. Surface observations also suggest that low level winds on the inflow side of the storm backed gradually, increasing the land track along the trajectory of the inflow. Some evidence for this can also be observed in the radar rainfall rate sequences. From about 0200 UTC, a weak echo channel is visible running northwest from the coastline towards the storm core (see 0200 UTC panel in Figure 8). This likely marks the location of strongest inflow into the storm at this time. By 0230 UTC, this feature had moved north and had rotated cyclonically, being almost cut off

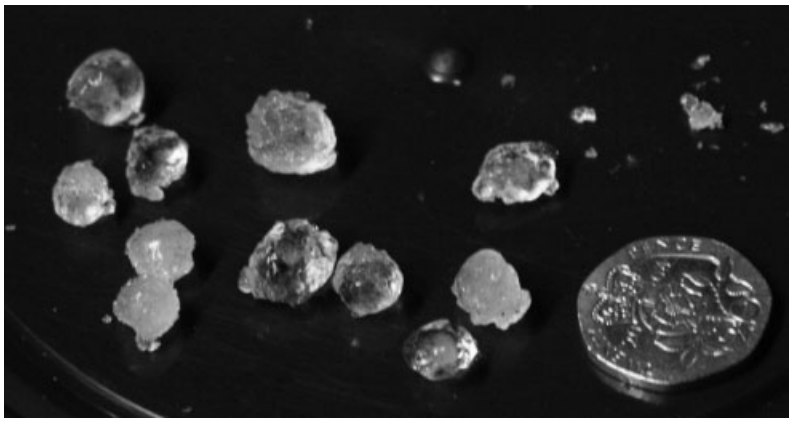

Figure 11. Sample of the larger hailstones collected from the area between Ottery St Mary and West Hill, near the centre of the storm path.

from the moist plume which by this time was located over Lyme Bay.

One of the most unusual aspects of the Ottery St Mary storm, in addition to the extreme rainfall totals, was the copious quantity of small hail that the storm generated. Visual inspection of hail deposits after the event revealed the maximum hail diameter to be a little less than 10 mm, though the vast majority of stones were nearer 5 mm in diameter. The hail was spherical or near spherical, and was 'hard' hail rather than graupel or 'soft hail'. Some of the larger stones were observed to exhibit an opaque centre with a single, clear outer layer, whilst others appeared either transparent or translucent throughout (see Figure 11). Clear ice is indicative of wet growth, in which freezing is slow and hence any trapped air can escape, producing a higher density stone. The opaque cores suggest that graupel may have formed the nuclei of many of the larger stones however. Although a rigorous study of the causes of hail generation within the storm is beyond the scope of this study, some clues as to how the storm produced so much hail may be found in the available observational data. Firstly, surface temperatures were only a few degrees Celsius above freezing, and consequently melting of small hailstones as they fell to ground would have been minimized. Small hail (*ca* 5 mm diameter) is not an uncommon phenomenon in the cool season in the United Kingdom when showery polar maritime airstreams are present, particularly close to windward coasts. This is primarily a consequence of steep lapse rates, caused by warming of the lowest layers of the cool airmass by passage over relatively warm sea surface temperatures, and cool airmass temperatures with a relatively low freezing level. In this case, the tephigram generated from the 0000 UTC Camborne ascent (Figure 6) shows lapse rates were particularly steep (approaching the dry adiabatic lapse rate) in two layers; the lower layer between 900 and 800 hPa and the upper layer between 650 and 550 hPa, as discussed previously. It is also interesting to note that over 70% of the cloud depth and the vast majority of CAPE were located within the temperature range corresponding to the mixed phase of water, in which super-cooled liquid water and solid hydrometeors may co-exist (i.e. parcel temperatures between 0 and about $-40\,^{\circ}$C).

The observed vertical wind profile may also help to explain how the storm was able to generate large amounts of small hail. At 0100 UTC, a moderately strong (though decreasing) westerly wind was observed above 2.5 km. This resulted in a component of flow directed towards the southeast side of the convective line, in the layer between about 3 and 6 km AGL. Within the upper half of this layer, temperatures were between -20 and $-35\,^{\circ}$C. Although super-cooled water may exist at temperatures as low as $-40\,^{\circ}$C, in practice at temperatures below -25 to $-30\,^{\circ}$C, the total cloud water content (i.e. solid and liquid) tends to be dominated by the ice content (Mazin, 2006). It is therefore probable that many solid hydrometeors would have been advected towards the southeastern edge of the storm system within this layer. These hydrometeors would tend to descend on the southeast side of the storm after leaving the main updraft. However, after falling some distance they would be advected back towards the centre of the convective line as they encountered the strong southeasterly inflow at lower levels, present on this side of the storm system. In this way, it is possible that updrafts of cells along the line were seeded at lower levels with many solid hydrometeors, which could then grow by collision with super-cooled liquid water droplets present within the lower-level updraft. Figure 12 is a schematic cross-section through the storm, in the northwest to southeast plain (approximately normal to the long axis of the convective system) at 0100 UTC. The hydrometeor trajectories discussed above are illustrated, based on the vertical profile of the convective line-normal component of flow (as shown on the right hand side of Figure 12). It should be noted that the hydrometeor trajectories, although congruent with available observations, are somewhat speculative. A modelling study which takes into account the relevant cloud microphysics and calculated fall-speeds would be desirable to further investigate factors leading to the hail production and distribution within the storm; this is however beyond the scope of the present study.

Whilst Figure 12 shows two dimensional trajectories, wind profiler data suggests that they would also have has

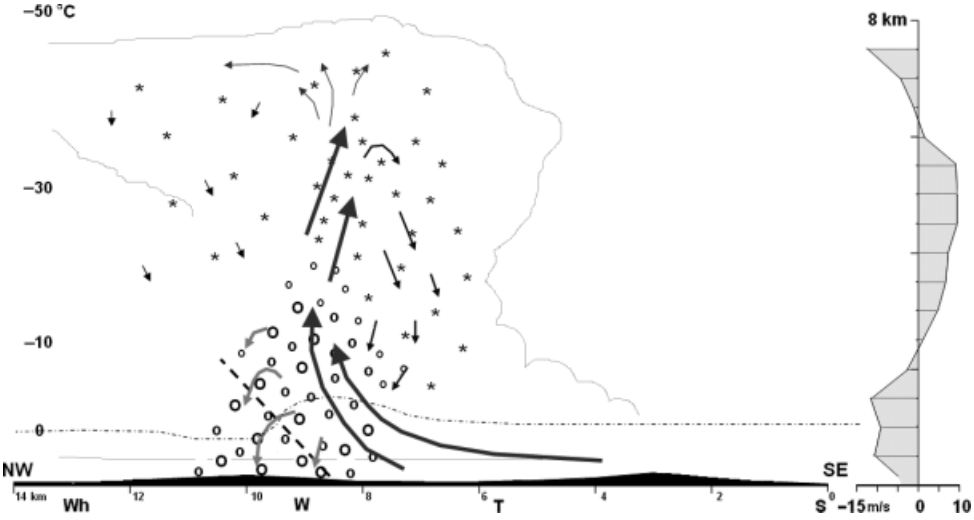

Figure 12. Schematic vertical cross section at 0100 UTC, in the northwest-southeast plain (approximately normal to the long axis of the convective system). Arrows show possible hydrometeor trajectories within the storm, based on the vertical profile of storm relative winds in the northwest-southwest plain (shown on right hand side). Asterisks represent solid hydrometeors (excluding hail) and circles represent hail. Vertical temperature profile (shown on left hand side) is based on the 0000 UTC Camborne radiosonde data. Thin dashed line denotes approximate freezing level. Bold dashed line shows approximate location of observed low-level wind shift and convergence line. On the horizontal axis, letters denote the locations of selected towns and villages; S = Sidmouth, T = Tipton St John, W = West Hill and Wh = Whimple.

some line-parallel (i.e. southwest-northeast orientated) component of motion. In a ground relative reference, mid- and upper-level winds in the system-parallel direction were rather weak at this time. However, since cells moved northeast along the line, cell-relative motion would be towards the southwest. Three dimensional cell-relative hydrometeor trajectories might, therefore, be envisaged as being helical, with solid hydrometeors originating at upper levels within a given cell advecting southwestward relative to that cell, owing to line-parallel cell relative flow, whilst also tending to advect southeastward owing to line-normal relative flow as they descended, before being caught in the updraft on the eastern edge of the neighbouring cell along the line, to the southwest. This motion may have helped to maintain a supply of solid hydrometeors, from which hailstones could grow, closer to the core of the convective system as the individual cells moved northeast. This may explain how hail-fall occurred continuously for such a prolonged period in a very restricted area close to the storm core, and how such large quantities of hail were able to fall very locally. If the line parallel flow in middle to upper levels was towards the northeast, the hail swathe might perhaps be expected to be more elongated in the northeast-southwest direction, but with smaller peak hail fall depths, all other factors being equal.

9. Conclusions

The analyses presented here show that a persistent, intense, quasi-stationary convective system was responsible for the exceptional rain- and hail-fall event over east Devon on 30 October 2008. The system developed in response to persistent, focussed low-level forced ascent, resulting from marked low-level convergence and moisture convergence in the vicinity of a small surface mesolow, which formed within an increasingly convectively unstable environment. Updraft rates resulting from the low-level convergence were likely on the same order of magnitude as those associated with the parcel buoyancy alone. Feedback mechanisms such as local surface pressure falls associated with latent heat release and additional focussing of convergence by convective downdrafts may have further enhanced the intensity and increased the longevity of the storm. Since the mesolow was slow moving, the location of the maximum in low-level convergence and moisture convergence was also slow moving, and persistent convection therefore affected a small area for an unusually prolonged period. Extreme rainfall totals in this case occurred primarily due to the resulting long duration of intense precipitation. However, the strong low level convergence, in addition to the CAPE, appears to have compensated for low total PW content, allowing rainfall rates to become very high given the relatively dry environment. There is no evidence, however, that the observed instantaneous rainfall rates were exceptional in themselves.

The value of observations for the post-analysis of small-scale convective events is illustrated by the results contained herein. However, it is interesting to further consider whether such observations could also provide any useful guidance in real time, to aid in the short term forecasting (0–6 h; i.e. ‘nowcasting’) of such events. High resolution models show considerable promise in terms of ability to identify the risk of such events over regions perhaps as small as one county in size: indeed, the Met Office 1.5 km model highlighted parts of Devon as being at risk of 3 h totals up to 90 mm in this case, as discussed by Grahame *et al*. (2009). However, it is still not easy to distinguish an unusual

event from an exceptional one. Nor is it easy to predict specific locations most likely to be affected with high confidence, owing to run-to-run variations, for example. In this case the inspection of manually generated analyses of surface observations hinted at areas of increased convective potential within the broader area identified by the high resolution models as being at risk of large rainfall totals, i.e. those areas characterized by locally higher surface dew point temperatures and strong low-level convergence. Some of these indicators were in evidence a number of hours before the flood event occurred over east Devon, as has been mentioned. Whilst this evidence could not possibly have been used to predict an exceptional event on its own, it could potentially have aided in the decision-making process associated with the location and timing of warning issuance, for example and the focussing of forecasters' attention to developments occurring within specific parts of the larger area defined as being at risk according to model output. The analysis here shows that continued monitoring of observations in this area of interest, once identified, revealed the continued deepening of the mesolow, together with its decreasing translational speed, both of which might have hinted at an increasing risk of prolonged convective rainfall at locations within its vicinity.

In this case, the existing surface synoptic observations network was only barely able to resolve the pertinent mesoscale features. For this reason, available automated surface analysis tools failed to resolve the mesolow properly and its intensity, and consequently the associated convergence and moisture convergence maxima could not have been inferred from the analyses. As a result the potential benefits of the surface observations for short term forecasting could not be fully realized. The use of private observations helped in the post-event analysis, allowing a clearer picture to be gained. However, private observations would not generally be available in real time to the forecaster. Doppler radar data also aided significantly in this case, as they resolved the mesolow and its low level wind field. However, the use of a wider variety of observations including Doppler radar data would necessitate rapid synthesis by the forecaster of a large amount of data, something which may not be practical within an operational environment, especially in situations with multiple regions of concern (which was, in fact, the case on this occasion, owing to a snow risk in association with the occlusion rain band further north over Wales and the Midlands).

Whilst general conclusions should not be drawn from one event, there is much evidence elsewhere in the literature that the location of initiation of severe convective events, and indeed deep convection in general, is often tied to small scale and sometimes subtle variations in surface parameters including temperature, dew point temperature and convergence (e.g. Wilson and Schreiber, 1986; Sanders and Doswell, 1995; Banacos and Schultz, 2005). Therefore high resolution observations of these parameters are crucial for the effective nowcasting of these events. Part of the solution may be to increase the density of surface observations, which would increase the likelihood of the automated surface analyses tools resolving the pertinent mesoscale features. This study suggests that maximum benefit would still require the simultaneous analysis of other available observations, including radar and wind profiler observations, however. If the aforementioned problems could be overcome, it seems that the maximum additional benefit could be derived from frequent, complete and timely analysis of all available observations, particularly in situations where the high resolution models have already identified a risk of severe weather.

Acknowledgements

The author would like to thank members of the public who provided eyewitness accounts and meteorological data recorded during the Ottery St Mary storm, both of which aided in the analysis of this event. Particular thanks are due to Nick Gardner, and to Chris Wilson and other members of the Norman Lockyer Observatory, Sidmouth. Thanks are also due to Malcolm Kitchen, Met Office, for reviewing an earlier draft of this paper.

References

Austin PM. 1987. Relation between measured radar reflectivity and surface rainfall. *Monthly Weather Review* **115**: 1053–1070.

Banacos PC, Schultz DM. 2005. The use of moisture flux convergence in forecasting convective initiation: historical and operational perspectives. *Weather and Forecasting* **20**: 351–366.

Corfidi SF. 2003. Cold pools and MCS propagation: forecasting the motion of downwind developing MCSs. *Weather and Forecasting* **18**: 997–1017.

Corfidi SF, Merritt JH, Fritsch JM. 1996. Predicting the movement of mesoscale convective complexes. *Weather and Forecasting* **11**: 41–46.

Fulton RA, Breidenbach JP, Seo DJ, Miller DA, O'Bannon T. 1998. The WSR-88D rainfall algorithm. *Weather and Forecasting* **13**: 377–395.

Georgiev CG. 1999. Quantitative relationship between Meteosat WV data and positive potential vorticity anomalies: a case study over the Mediterranean. *Meteorological Applications* **6**: 97–109.

Golding BW, Hand WH, Dent J, Dale M, Collier CG, Moore RJ, Cole SJ, Bell VA, Jones DA. 2007. Extreme event recognition Phase 2. R&D Technical Report FD2208/TR, Joint DefraEA Flood and Coastal Erosion Risk Management R&D Programme. DEFRA: London; pp. 29.

Grahame N, Riddaway B, Eadie A, Hall B, McCallum E. 2009. Exceptional hailstorm hits Ottery St Mary on 30 October 2008. *Weather* **64**: 255–263.

Maddox RA, Canova F, Hoxit LR. 1980. Meteorological characteristics of flash flood events over the western United States. *Monthly Weather Review* **108**: 1866–1877.

Maddox RA, Hoxit LR, Chappell F, Caracena F. 1978. Comparison of meteorological aspects of the big thompson and rapid city flash floods. *Monthly Weather Review* **106**: 375–389.

Mazin IP. 2006. Cloud phase structure: experimental data analysis and parameterization. *Journal of the Atmospheric Sciences* **63**: 667–681.

Met Office. 2008. Hail/thunderstorms over east Devon – 29/30 October 2008, www.metoffice.gov.uk/climate/uk/interesting/oct2008/ (accessed 25/08/2009).

Rotunno R. 1981. On the evolution of thunderstorm rotation. *Monthly Weather Review* **109**: 577–586.

Sanders FS, Doswell CA III. 1995. A case for detailed surface analysis. *Bulletin of the American Meteorological Society* **76**: 505–521.

Wilson JW, Schreiber WE. 1986. Initiation of convective storms at radar-observed boundary-layer convergence lines. *Monthly Weather Review* **114**: 2516–2536.